

Article

Study of Rock Mass Rating (RMR) and Geological Strength Index (GSI) Correlations in Granite, Siltstone, Sandstone and Quartzite Rock Masses

Gabor Somodi ¹, Neil Bar ², László Kovács ³, Marco Arrieta ², Ákos Török ⁴  and Balázs Vásárhelyi ^{4,*}¹ Hidro-Duna Ltd., HU-2541 Lábatlan, Hungary; somodigabor@gmail.com² Gecko Geotechnics, Cairns, QLD 4870, Australia; neil@geckogeotech.com (N.B.); marco@geckogeotech.com (M.A.)³ RockStudy Ltd. (Kőmérő Kft.), HU-7633 Pécs, Hungary; kovacsaszlo@komero.hu⁴ Department Engineering Geology and Geotechnics, Budapest University of Technology and Economics, HU-1111 Budapest, Hungary; torok.akos@emk.bme.hu

* Correspondence: vasarhelyi.balazs@emk.bme.hu

Abstract: A comprehensive understanding of geological, structural geological, hydrogeological and geotechnical features of the host rock are essential for the design and performance evaluation of surface and underground excavations. The Hungarian National Radioactive Waste Repository (NRWR) at Bataapáti is constructed in a fractured granitic formation, and Telfer Gold Mine in Australia is excavated in stratified siltstones, sandstones and quartzites. This study highlights relationships between GSI chart ratings and calculated GSI values based on RMR rock mass classification data. The paper presents linear equations for estimating GSI from measured RMR₈₉ values. Correlations between *a* and *b* constants were analyzed for different rock types, at surface and subsurface settings.



Citation: Somodi, G.; Bar, N.; Kovács, L.; Arrieta, M.; Török, Á.; Vásárhelyi, B. Study of Rock Mass Rating (RMR) and Geological Strength Index (GSI) Correlations in Granite, Siltstone, Sandstone and Quartzite Rock Masses. *Appl. Sci.* **2021**, *11*, 3351. <https://doi.org/10.3390/app11083351>

Academic Editor: Tivadar M. Tóth

Received: 28 February 2021

Accepted: 6 April 2021

Published: 8 April 2021

Publisher's Note: MDPI stays neutral with regard to jurisdictional claims in published maps and institutional affiliations.



Copyright: © 2021 by the authors. Licensee MDPI, Basel, Switzerland. This article is an open access article distributed under the terms and conditions of the Creative Commons Attribution (CC BY) license (<https://creativecommons.org/licenses/by/4.0/>).

Keywords: rock mass classification; RMR; GSI; granite; sandstone; quartzite

1. Introduction

In most aspects of deep surface and underground excavations, the focus of geological and geotechnical investigations is on understanding rock mass properties, including the mechanical properties of intact rock and discontinuities as well as the geometry and orientation of discontinuities. These conditions are evaluated according to the size of the excavation, its geometry, and available rock mass data.

Individual components of rock mass classification systems define intact rock and discontinuity characteristics as well as the orientation of discontinuities relative to an excavation and fracture frequency. Special care is required to avoid sample bias, and in most cases, discontinuity (e.g., joint) lengths can be crudely estimated by observing the discontinuity trace lengths on surface exposures [1]. The parameters of the rock mass classification systems must reflect actual ground conditions and consider their effect on the stability of the proposed excavation.

In this study, the mechanical response of the rock mass forms an essential part of understanding the behaviour of the granitic host rock at a deep underground radioactive waste disposal site (Hungary). Similarly, understanding rock mass parameters is key to assessing the stability of deep rock slope excavations at a large open pit gold mine in Australia. Scale effects, anisotropy, and confining stresses influence the rock mechanical problems, especially in geomechanics simulations [2,3]. Modelling requires geometric data regarding fracture size distribution, spatial density, and orientation. Afterwards, simulated models are available to understand features of the fractured rock body concerning hydrodynamic behaviour (e.g., connectivity, porosity, and permeability) [4] and mechanical behavior (i.e., shear strength of fractures, elastic parameters of rock mass).

Rock masses can be described using standardized descriptors and quantitative parameters associated with those descriptors, as engineers feel more confident with numbers. In this context, rock mass classification systems represent an attempt to “put numbers to geology” [5].

Various rock mass classifications have appeared since the beginning of the 20th century. Some of these include the classification system of Protodyaknov [6], of Terzaghi [7], the RQD [8], the RSR [9], the RMR [10], Q-system [11], GSI [12], RMI [13], and some recent ones such as the Rock Mass Fabric Indices (F) [14] and the Rock Mass Quality Index [15]. At this point, it should be mentioned that RMR and the Q-system have been the most widely used methods (Palmström [16]; Ranassoriya and Nikraz [17]; Fernández-Gutierrez et al. [18]). However, other classifications such as RMI and GSI have been attracting more interest in recent years.

The Rock Mass Rating (RMR) classification system was developed by Bieniawski [10] in 1973, and after several modifications, the 1989 version is the most used in rock engineering practice [19]. This classification system has been refined over several years, and its characterization method has been revised from its creation onward. The last modification of this classification system was introduced in 2014 [20].

The Geological Strength Index (GSI) system is widely used for estimating the strength reduction from an intact rock to a rock mass, introduced by Hoek [12] in 1994. It is a unique rock mass classification system used as part of the Hoek–Brown failure criterion for estimating the strength and stiffness of a rock mass [21,22]. Accurate estimation of the GSI is important for subsequent calculations [23,24]. As in other rock mass classifications, all the GSI-based equations are highly sensitive to their respective input parameters [25]. Figure 1 presents a chart for estimating GSI for jointed rock masses in the field.

GEOLOGICAL STRENGTH INDEX FOR JOINTED ROCKS	SURFACE CONDITIONS				
	VERY GOOD	GOOD	FAIR	POOR	VERY POOR
STRUCTURE	DECREASING SURFACE QUALITY →				
 INTACT OR MASSIVE—intact rock specimens or massive in situ rock with few widely spaced discontinuities	90				
 BLOCKY—well interlocked undisturbed rock mass consisting of cubical blocks formed by three intersecting discontinuity sets	80				
 VERY BLOCKY—interlocked, partially disturbed mass with multi-faceted angular blocks formed by 4 or more joint sets	70				
 BLOCKY/DISTURBED/SEAMY—folded with angular blocks formed by many intersecting discontinuity sets. Persistence of bedding planes or schistosity	60		40		
 DISINTERATED—poorly interlocked, heavily broken rock mass with mixture of angular and rounded rock pieces				20	
 LAMINATED/SHEARED—Lack of blockiness due to close spacing of weak schistosity or shear planes					10

Figure 1. Chart for determining the geological strength index (GSI) of jointed rock mass [21].

For practical engineering application, the Hoek–Brown failure criterion should only be applied when the potential for structurally controlled failures has been eliminated, as it treats the rock mass as an isotropic material.

The use and limitation of several rock mass characterization approaches are described and studied through surveyed data [26] and the results of some recent publication.

Although there are various rock mass classifications, not one of them has prevailed over another, and normally, the use of more than one classification is highly recommended,

even by their respective authors (Bieniawski [19], Palmström [16]). Since the first correlation between RMR and the Q-system, proposed by Bieniawski [27], many correlations have been proposed from tunnel and mine projects all over the world [28–30]. Moreover, when correlations are applied to the same rock lithology, better results are obtained [31–33].

The goal of this research is to prepare a comparative study to understand parameter sensitivity and differences between methods of rock mass characterization. The results help to understand relationships from mapping results from site investigations in different locations, excavation types and ground conditions, i.e., an open pit gold mine and the construction of a nuclear waste repository. This, in turn, assists in understanding potential gaps and sources of error when correlations are used, e.g., estimated from drill core data.

2. Research Methodology and Research Materials

Determination of GSI and RMR₈₉

GSI can be estimated for an exposed rock slope or tunnel face using the standard chart and field observations of rock mass blockiness and surface condition of the discontinuity (see Figure 1). Other charts are available for different rock masses (e.g., flysch, foliated, etc.).

Several independent quantitative theories were developed for the estimation of GSI values from drill core data. This has been used in cases when rock exposures, tunnel faces or slopes were not yet available (e.g., initial feasibility studies prior to excavation). Different rock mass classification systems have been utilized in the approach to correlate drill core data to GSI, and include the following:

- Q-system-based calculation method (e.g., [34,35])
- RMI-based calculation method (e.g., [36,37])
- RMR-based calculation method (e.g., [21,35])

Several authors [26,38–40] have theoretically shown that significant differences in GSI estimation result from applying different calculation methods for different rock types.

This paper focuses on calculated estimations of GSI from Rock Mass Rating (RMR) values. Recently, several researchers have investigated the relationship between Bieniawski's [19] Rock Mass Rating (RMR₈₉) and the GSI. Firstly, [21,33] suggested the following calculation:

$$\text{GSI} = \text{RMR}_{89} - 5 \text{ for } \text{RMR}_{89} > 23 \quad (1)$$

In this equation, RMR₈₉ can be calculated from the following parameters:

$$\text{RMR}_{89} = R1 + R2 + R3 + R4 + R5 \quad (2)$$

where:

- R1—uniaxial compressive strength (0–15),
- R2—rock quality designation, RQD (3–20),
- R3—average joint space (5–20),
- R4—joint wall conditions (0–30), and
- R5—water. In the original definition, R5 must be defined as dry (i.e., 15) for assessing drill core.

Based on further studies, Hoek et al. [35] suggested the following simple formula for GSI calculation:

$$\text{GSI} = 0.5 \text{ RQD} + 1.5 J_c \quad (3)$$

where J_c is the joint wall conditions, according to the definition of Bieniawski [19] and it is equal to the R4 value of the previous equation, thus the rate of it is between 0 and 30.

Similarly, Hoek et al. [22,33] and several authors have recommended estimating the GSI value from RMR₈₉ using a linear equation in the form of

$$\text{GSI} = a \text{ RMR}_{89} + b \quad (4)$$

where a and b are different constants, depending on the rock type or geographical location. Table 1 summarizes various constants that have been calculated in previous works.

Table 1. Equations of the existing correlations between RMR₈₉ and GSI.

	a	b	R ²	Rock Type	Ref.
1	1.00	−5		various projects	Hoek et al. [22]
2	0.42	23.08	0.44	schist and sedimentary rocks	Cosar [41]
3	0.739	12.097	0.759		sandstone
4	0.7394	−4.3349	0.57	metamorphic	Singh and Tamrakar [43]
5	0.9932	−4.913	0.84	gabbro, ultrabasic	Ali et al. [44]
6	1.2092	−18.6143		various projects	Zhang et al. [45]
7	1.265	−21.49		various types of rocks	Siddique and Khan [46]

In case of poor and very poor rock mass (i.e., RMR < 30) Osgoui and Ünal [47] suggested an exponential relationship for calculating the GSI value from RMR₈₉:

$$GSI = 6e^{0.05RMR_{89}} \tag{5}$$

The suggested equations (using the constants presented in Table 1) are summarized in graphic form (Figure 2). Reviewing the results, it is evident that the equation of Osgoui and Ünal [47] is the only one focusing on RMR₈₉ below 30. The results also suggest that equations by Cosar [41] and Singh and Tamarkar [43] underestimate GSI for RMR₈₉ > 30 when compared to the others. The remaining five formulae converge with similar results between RMR₈₉ values of 60 and 70, while drifting apart above and below. As illustrated in Figure 2, the highest variability between equations occurs when RMR₈₉ < 30, and when RMR₈₉ > 80. These represent rock masses at opposite ends of the spectrum, those of very poor, and very good quality.

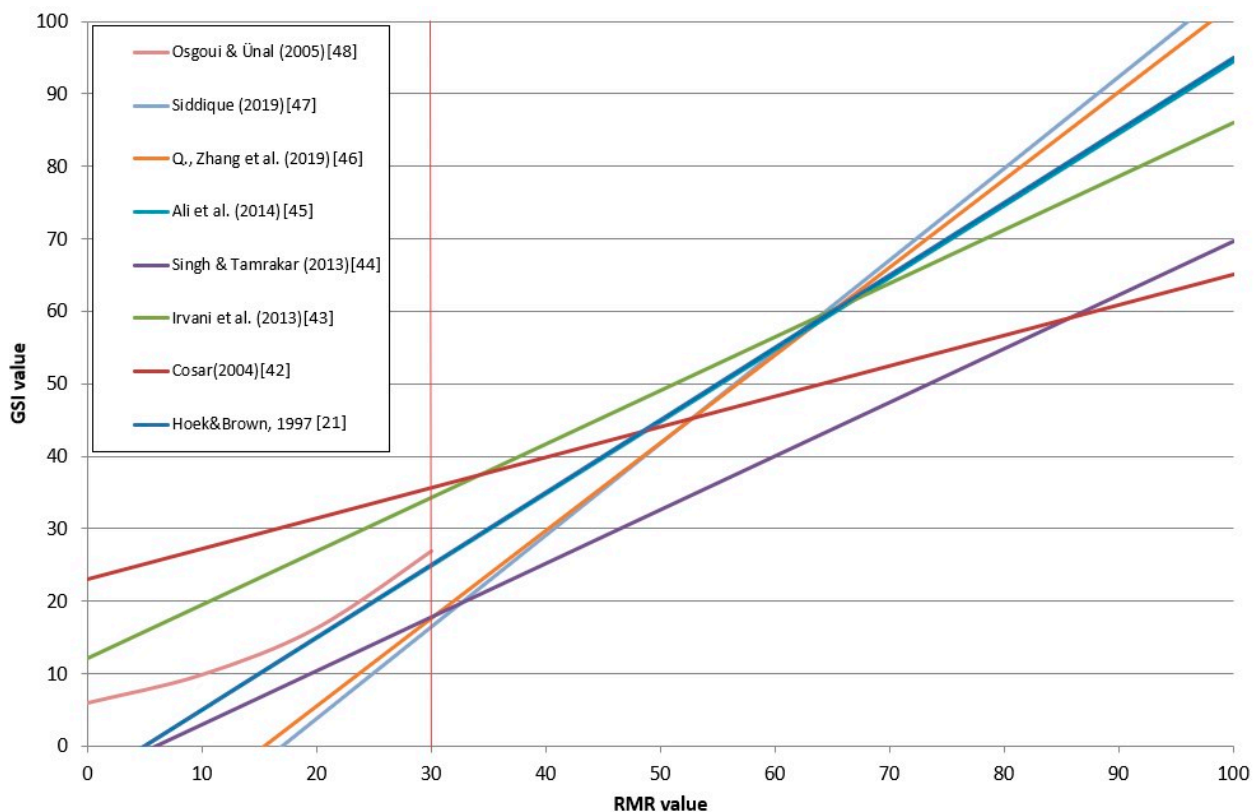


Figure 2. Existing correlations between RMR₈₉ and GSI listed in Table 1.

3. Geological Setting and Database

3.1. Geological Setting and Data of Hungarian Nuclear Waste Repository

The research areas comprise granitic rock masses near Bábaapáti in Hungary and anisotropic siltstones, sandstones, and quartzite in Western Australia.

The fractured granitic body forms the host rock of the Hungarian National Radioactive Waste Repository (NRWR). Until now, a more than 6 km long tunnel network has been constructed, and all the tunnel faces have been documented [4,48]. From a geological aspect, three main rock types can be distinguished in the carboniferous granite formation: monzogranite, monzonite, and hybrid rocks [3,49]. This granitic body is transected by Cretaceous trachyandesite dykes with NE–SW strike and randomly distributed aplitic veins also [50]. The four repository chambers were excavated in monzogranite with aplitic veins and scarce monzonite enclaves.

The results of previous field observations and models suggested that the granite formation is hydraulically strongly compartmented, dividing the underground flow system into several blocks of limited hydraulic connection. Based on field observations, it was distinguished as less transmissive blocks bordered by more transmissive zones. The repository for low and medium level nuclear waste disposal is placed in a less transmissive hydraulic compartment [51,52]. Based on measured geometric data (spatial position, length, orientation, and aperture), fracture networks are simulated to study connectivity relations and for computing the fractured porosity and permeability at different scales. The results prove the scale-invariant geometry of the fracture system [4,53]. Geotechnical data from drill core logging and tunnel face documentation show a clear connection between rock mass classification and rock type [26,49,50].

The database consists of two types of RMR₈₉ and GSI values: field values, which were estimated directly from slope or tunnel faces, and values back-calculated from other methods (e.g., GSI from RMR₈₉). The database covers the ratings from repository chambers and other tunnels with smaller cross-sections (Figure 3).

3.2. Geological Setting and Data of Telfer Gold Mine

A large gold deposit occurs within Proterozoic stratigraphy at the Telfer Gold Mine in the Great Sandy Desert of Western Australia. Rock types include calcareous and argillaceous siltstones, sandstones and quartzites. The geological structure is complex and is the primary reason behind the mineralization [54].

The properties of intact rock mass and rock mass shear strength, and to a lesser extent, bedding shear strength, vary with the degree of weathering and the type of alteration (clay or silica enrichment). Planar sliding along adversely oriented bedding planes within siltstone, sandstone and quartzite are the most common causes of slope instability.

Similarly to the Hungarian granitic rock masses, two types of data exist for Telfer: field values of GSI and RMR₈₉, estimated on-site based on observations from 12–24 m high slope faces (Figure 4), and calculated GSI values from drill core estimations of Q and RMR₈₉ [55].

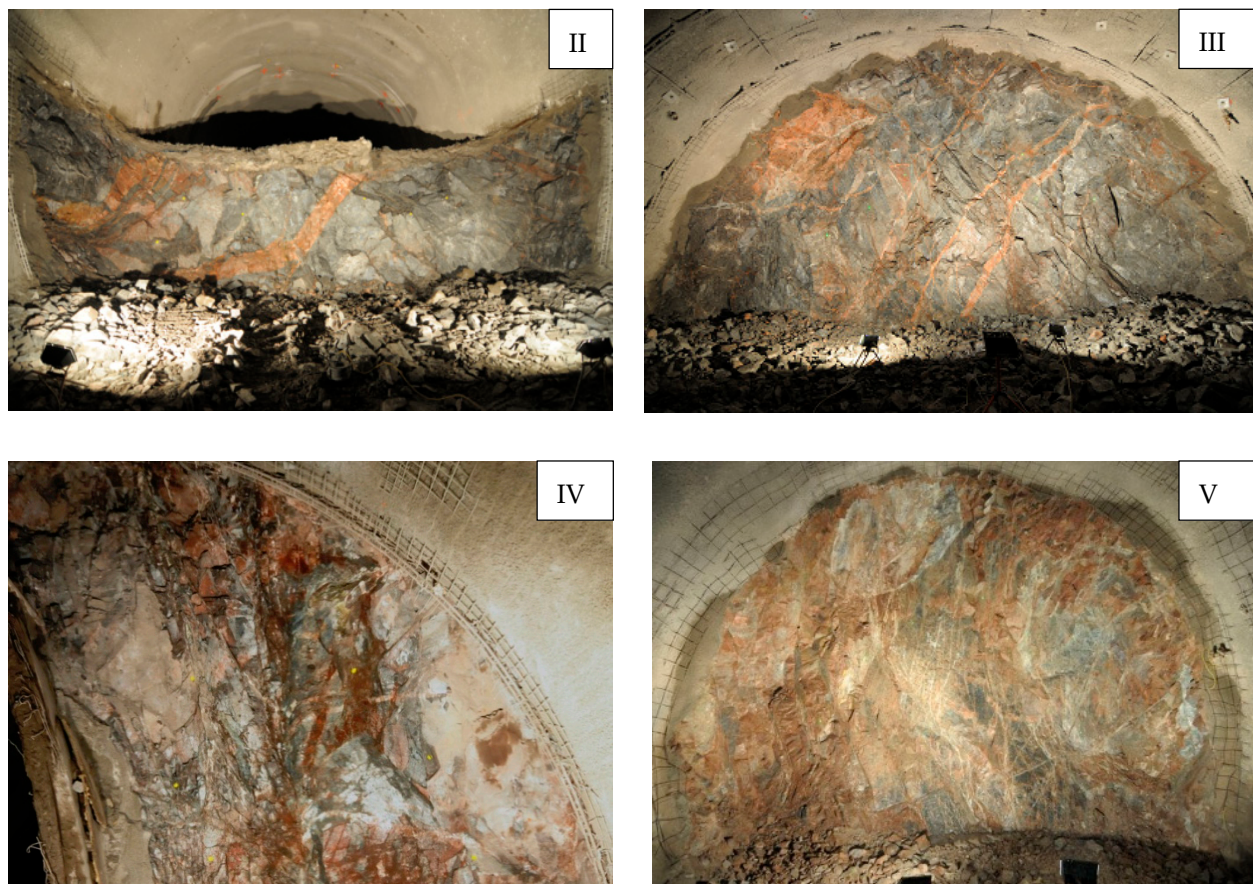


Figure 3. Examples of rock mass classes in various tunnel sections: Chamber bench $\sim 60 \text{ m}^2$ (class II), Chamber top heading $\sim 60 \text{ m}^2$ (class III), Chamber half top heading 30 m^2 (class IV), Research tunnel 33 m^2 (class V) (granitic rocks, Bataapati, Hungary).



Figure 4. (Left): near-laminated weathered siltstone with siltstone-siltstone bedding planes (Telfer Gold mine, Australia). (Right): planar failure in fresh quartzite with quartzite-quartzite bedding planes (Telfer Gold Mine, Australia). Both have bedding scale anisotropy [28].

4. Results and Discussion

4.1. Comparing the Calculated GSI Values to the Chart Values

Using the entire database, the two RMR-based different equations of GSI determination (Equations (1)–(5)) and GSI field values were analyzed, based on the observations

during the excavation of the Bataapáti radioactive waste repository. Using the two RMR-based equations, Equations (1) and (3), different correlations were found (Figures 5 and 6). Using Equation (1), the obtained values are always higher than the chart values (GSI_{chart}). There is a linear relationship between the two values:

$$GSI_{chart} = 0.793 GSI_{calc(1)} + 5.974 \quad (R^2 = 0.736) \quad (6)$$

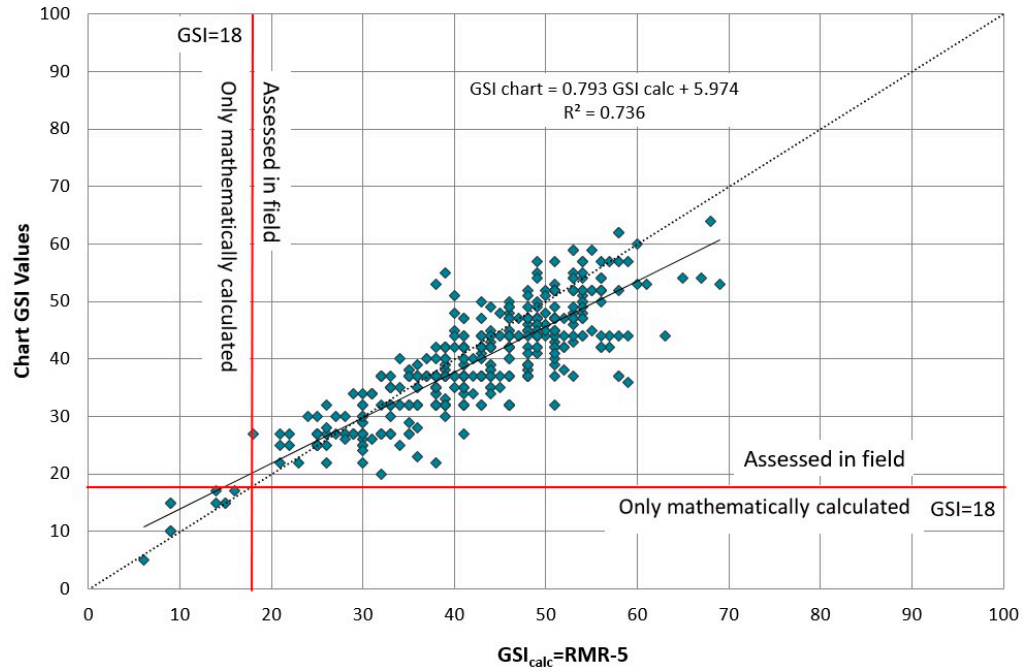


Figure 5. Correlations between Chart and calculated GSI values using Equation (1).

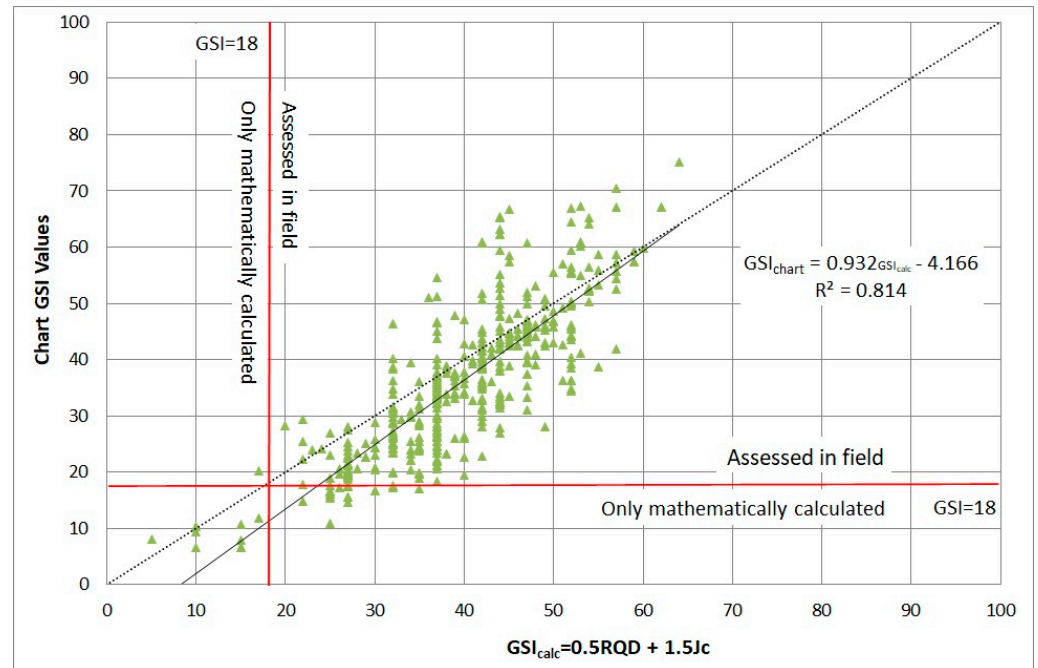


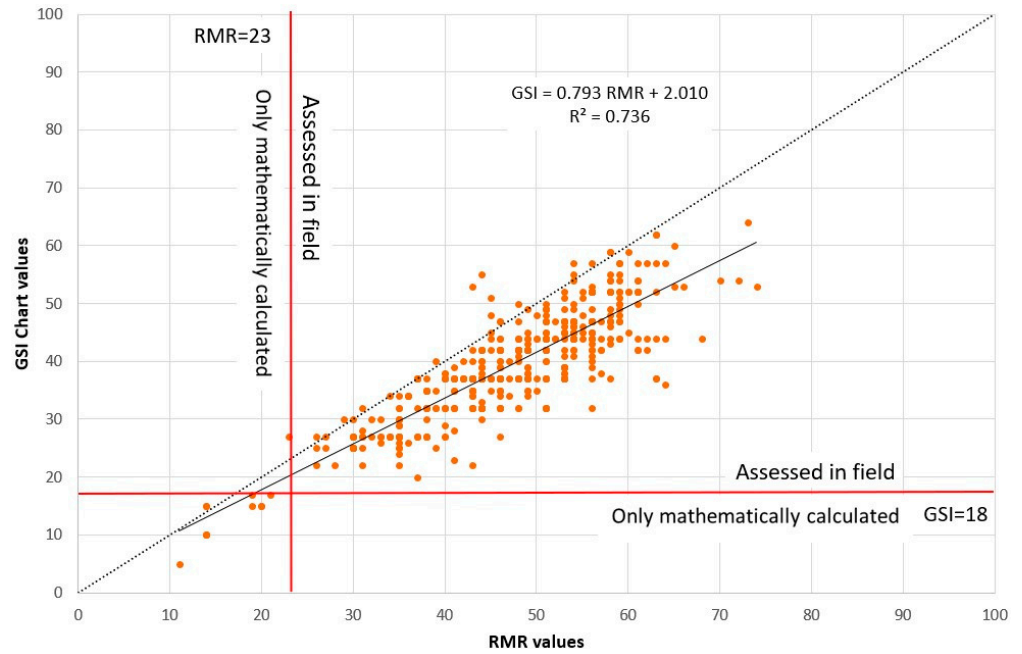
Figure 6. Correlations between Chart and calculated GSI values using Equation (3).

Using Equation (3), the calculated points are nearly equal to the chart points:

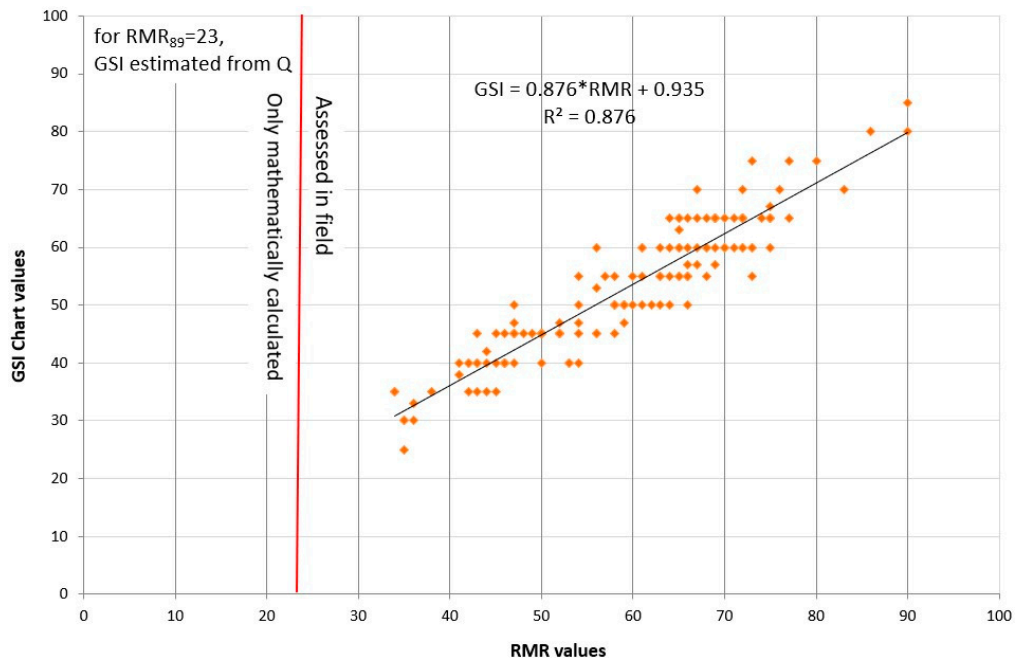
$$GSI_{chart} = 0.932 GSI_{calc(2)} - 4.166 \quad (R^2 = 0.814) \quad (7)$$

4.2. Comparing the RMR Value to the GSI Value

The chart Geological Strength Index is plotted as a function of RMR₈₉ values in Figure 7. According to the calculated results, the linear regression is shown in Table 2.



(a)



(b)

Figure 7. Correlation between Chart GSI and RMR values in Bataapati project (a), and in Telfer project (b).

Table 2. Equations of the existing correlations between RMR₈₉ and GSI in the studied projects.

a	b	R ²	Rock Type	Ref.
0.793	2.010	0.736	granitic rocks	Bátaapáti
0.876	0.935	0.876	siltstones, sandstones and quartzites	Telfer

The studied correlations show distinct connections between the two rock mass characterization methods. Good correlations between a and b constants from Equation (3) were identified in different projects.

The use of rock-type-based equations and constants from Table 1 did not identify a clear or discernible correlation between RMR₈₉ and GSI. However, further examination of the relationship between ‘a’ and ‘b’ constants indicate a strong correlation for individual cases. The connection between a and b constants obtained from Equation (4) are illustrated in Figure 8.

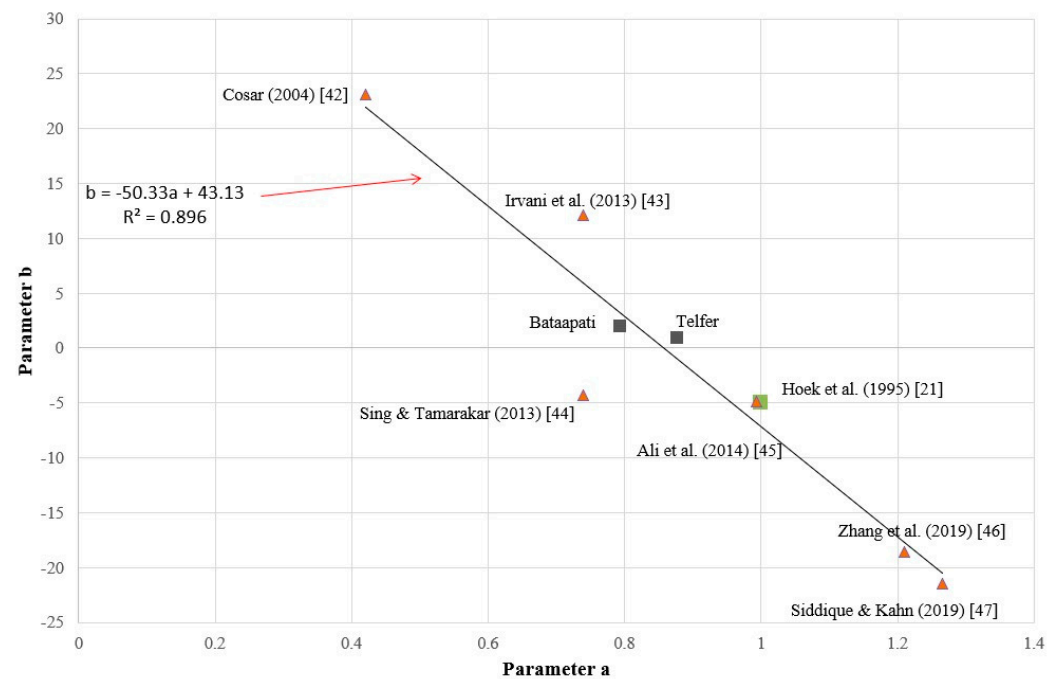


Figure 8. The correlation between different a and b constants regarding different correlations between GSI-RMR₈₉ values.

The calculated values from Hungary (Bátaapáti) and Australia (Telfer) from this paper are also shown in Figure 8. Constants a and b from Equation (4) can be correlated by:

$$b = -50.13a + 43.13 \quad (R^2 = 0.896) \tag{8}$$

This value is considered as site- and rock-type dependent.

In Figure 8, the various relationships appear to follow a linear relationship with the exception of published data by Singh and Tamarkar [43]. When these data are omitted, an even higher correlation is attained:

$$B = -53.77a + 47 \quad (R^2 = 0.977) \tag{9}$$

Using this latter Equation (9), a = 1, while b = -6.29. These values are commensurate to the values suggested by Hoek and Brown [33].

5. Conclusions

This study describes the relationship between Rock Mass Rating (RMR) and Geological Strength Index (GSI). Quantitative assessments of the correlations have been conducted systematically based on the available study data from Bátaapáti and Telfer on the correlations of primary classified indices of RMR and GSI.

The following simplified quantitative correlations between RMR₈₉ and GSI are proposed using large data sets:

$$\text{GSI} = 0.793 \text{ RMR}_{89} + 2.001 \quad (R^2 = 0.736, \text{ Bátaapáti}) \quad (10)$$

$$\text{GSI} = 0.876 \text{ RMR}_{89} + 0.935 \quad (R^2 = 0.876, \text{ Telfer}) \quad (11)$$

These two proposed quantitative correlations between RMR₈₉ and GSI are applied to evaluate the surrounding rock mass of the Bátaapáti site (granitic rock mass in Hungary) and Telfer Gold Mine (siltstones, sandstones and quartzites of Western Australia). Whilst they are likely applicable elsewhere in similar ground conditions, readers are strongly encouraged to validate these and other correlations at their local site prior to use.

The validated results demonstrate that the proposed simplified quantitative correlation reflects the observed relationship between RMR₈₉ and GSI.

To provide the input data for empirical design of excavations in tunnels or mining projects, it is necessary to determine the geological conditions in the study areas and carry out rock mass classifications to predict ground behavior. The obtained results can be also applied in other research fields such as geomechanics simulation, fracture network characterization and hydrological modelling. Based on these results, it can be concluded that an extensive data set of underground or surface settings provides a sound basis for rock mass classification of various lithologies.

Author Contributions: G.S. Writing—original draft preparation, L.K. and Á.T.; Formal and data collection analysis, N.B. and M.A.; Reviewing, methodology and data collection, B.V.; Conceptualization, investigation and methodology, editing. All authors have read and agreed to the published version of the manuscript.

Funding: This research was funded by National Research Development and Innovation Office of Hungary (Grant No. TKP2020 BME-IKA-VIZ and NKFIH 124366, NKFIH 124508) and the Hungarian-French Scientific Research Grant (No. 2018-2.1.13-TE T-FR-2018-00012).

Institutional Review Board Statement: Not applicable.

Informed Consent Statement: This paper has been published with the permission of Public Limited Company for Radioactive Waste Management (PURAM).

Data Availability Statement: 3rd Party Data.

Conflicts of Interest: The authors declare no conflict of interest.

References

1. Palmström, A. RMI—A Rock Mass Characterization System for Rock Engineering Purposes. Ph.D. Thesis, University of Oslo, Oslo, Norway, 1995; p. 400.
2. Deisman, N.; Chalaturnyk, R.; Mas, I.D.; Darcel, C. Geomechanical characterization of coal seam reservoirs: The SRM approach. In Proceedings of the Asia Pacific Coalbed Methane Symposium, Brisbane, Australia, 22–24 September 2008; pp. 1–10.
3. Kovács, L.; Mészáros, E.; Somodi, G. Rock Mechanical and Geotechnical Characterization of a Granitic Formation Hosting the Hungarian National Radioactive Waste Repository at Bátaapáti. In *Engineering Geology for Society and Territory, Volume 6: Applied Geology for Major Engineering Projects*; Springer: Berlin/Heidelberg, Germany, 2015; pp. 915–918.
4. Tóth, T.M. Fracture network characterization using 1D and 2D data of the Mórággy Granite body, southern Hungary. *J. Struct. Geol.* **2018**, *113*, 176–187. [[CrossRef](#)]
5. Hoek, E. Putting numbers to geology—An engineer's viewpoint. *Quart. J. Eng. Geol. Hydrogeol.* **1999**, *32*, 1–19. [[CrossRef](#)]
6. Protodyakonov, M.M. *Rock Pressure on Mine Support (Theory of Mine Support)*; Tipografiya Gubernskogo Zemstva: Yekaterinoslav, Russia, 1907; pp. 23–45.
7. Terzaghi, K. Rock defects and loads on tunnel supports. In *Rock Tunnelling with Steel Supports*; Proctor, R.V., White, T.L., Eds.; Commercial Shearing and Stamping Company: Youngstown, OH, USA, 1946; pp. 17–99.

8. Deere, D.U.; Hedron, A.J.; Patton, F.D.; Cording, E.J. Design of surface and near-surface construction in rock. In *Failure and Breakage of Rock, Proceedings of the 8th US Symposium on Rock Mechanics*; Fairhurst, C., Ed.; Society of Mining Engineers of AIME: New York, NY, USA, 1967; pp. 237–302.
9. Wickham, G.E.; Tiedemann, H.R.; Skinner, E.H. Support determinations based on geologic predictions. In *Proceedings of the North American Rapid Excavation and Tunnelling Conference*, Chicago, IL, USA, 5–7 June 1972; pp. 43–64.
10. Bieniawski, Z.T. *Engineering Classification of Jointed Rock Masses*; South African Institute of Civil Engineers: Johannesburg, South Africa, 1973; Volume 15, pp. 333–343.
11. Barton, N.; Lien, R.; Lunde, J. Engineering classification of rock masses for the design of rock support. *Rock Mech.* **1974**, *6*, 189–236. [[CrossRef](#)]
12. Hoek, E. Strength of rock and rock masses. *ISRM News J.* **1994**, *2*, 4–16.
13. Palmstrom, A. Characterizing rock masses by the RMI for use in practical rock engineering, Part 2: Some practical applications of the Rock Mass index (RMI). *Tunn. Undergr. Space Technol.* **1996**, *11*, 287–303. [[CrossRef](#)]
14. Tzamos, S.; Sofianos, A.I. A correlation of four rock mass classification systems through their fabric indices. *Int. J. Rock Mech. Min. Sci.* **2007**, *44*, 477–495. [[CrossRef](#)]
15. Aydan, Ö.; Ulusay, R.; Tokashiki, N. A new rock mass quality rating system: Rock Mass Quality Rating (RMQR) and its applications to the estimation of geomechanical characteristics of rock masses. *Rock Mech. Rock Eng.* **2014**, *47*, 1255–1276. [[CrossRef](#)]
16. Palmström, A. Combining the RMR, Q, and RMI classification systems. *Tunn. Undergr. Space Technol.* **2009**, *24*, 491–492. [[CrossRef](#)]
17. Ranasooriya, J.; Nikraz, H. Reliability of the linear correlation of Rock Mass Rating (RMR) and Tunnelling Quality Index (Q). *Aust. Geomech.* **2009**, *44*, 47–54.
18. Fernández-Gutierrez, J.D.; Pérez-Acebo, H.; Mulone-Andere, D. Correlation between Bieniawski’s RMR index and Barton’s Q index in fine-grained sedimentary rock formations. *Inf. Construcción* **2017**, *69*, e205.
19. Bieniawski, Z.T. *Engineering Rock Mass Classification*; Wiley: New York, NY, USA, 1989.
20. Celada, B.; Tardáguila, I.; Varona, P.; Rodríguez, A.; Bieniawski, Z.T. Innovating Tunnel Design by an Improved Experience-based RMR System. In *Proceedings of the World Tunnel Congress 2014—Tunnels for a Better Life*, Foz do Iguaçu, Brazil, 9–15 May 2014.
21. Hoek, E.; Kaiser, P.K.; Bawden, W.F. *Support of Underground Excavations in Hard Rock*; AA Balkema: Rotterdam, The Netherlands, 1995.
22. Hoek, E.; Brown, E.T. The Hoek-Brown Failure criterion and GSI. *J. Rock Mech. Geotechnol. Eng.* **2019**, *11*, 445–463. [[CrossRef](#)]
23. Vásárhelyi, B.; Kovács, D. Empirical methods of calculating the mechanical parameters of the rock mass. *Period. Polytech. Civil Eng.* **2017**, *61*, 39–50.
24. Hussian, S.; Mohammad, N.; Rehman, Z.U.; Khan, N.M.; Shahzada, K.; Ali, S.; Tahir, M.; Raza, S.; Sherin, S. Review of the Geological Strength Index (GSI) as an Empirical Classification and Rock Mass Property Estimation Tool: Origination, Modifications, Applications, and Limitations. *Adv. Civil. Eng.* **2020**, 6471837. [[CrossRef](#)]
25. Ván, P.; Vásárhelyi, B. Sensitivity analysis of GSI based mechanical parameters of the rock mass. *Period. Polytech. Civil Eng.* **2014**, *58*, 379–386. [[CrossRef](#)]
26. Vásárhelyi, B.; Somodi, G.; Krupa, Á.; Kovács, L. Determining the Geological Strength Index, GSI using different methods. In *Proceedings of the 2016 ISRM International Symposium (EUROCK2016)*, Ürgüp, Turkey, 29–31 August 2016; pp. 1049–1054.
27. Bieniawski, Z.T. Rock mass classification in rock engineering. In *Proceedings of the Symposium on Exploration for Rock Engineering*, Johannesburg, South Africa, 1–5 November 1976; pp. 97–106.
28. Rutledge, J.C.; Preston, R.L. Experience with engineering classifications of rock. In *Proceedings of the International Tunnel Symposium*, Tokyo, Japan, 29 May–2 June 1978; pp. A3.1–A3.7.
29. Moreno Tallon, E. Comparison and application of geomechanics classification schemes in tunnel construction. In *Proceedings of the Tunnelling ’82—3rd International Symposium*, Brighton, UK, 7–11 June 1982; pp. 241–246.
30. Sayeed, I.; Khanna, R. Empirical correlation between RMR and Q systems of rock mass classification derived from Lesser Himalayan and Central crystalline rocks. In *Proceedings of the International Conference on “Engineering Geology in New Millenium”*, New Delhi, India, 27–29 October 2015.
31. Castro-Fresno, D. Correlation between Bieniawski’s RMR and Barton’s Q index in low-quality soils. *Rev. Construcción* **2010**, *9*, 107–119. [[CrossRef](#)]
32. Campos, L.A.; Ferreira Filho, F.A.; Vieira Costa, T.A.; Gomes Marques, E.A. New GSI correlations with different RMR adjustments for an eastern mine of the Quadrilatero Ferrífero. *J. S. Am. Earth Sci.* **2020**, *102*, 102647. [[CrossRef](#)]
33. Hoek, E.; Brown, E.T. Practical estimates of rock mass strength. *Int. J. Rock Mech. Min. Sci.* **1997**, *34*, 1165–1186. [[CrossRef](#)]
34. Barton, N. The influence of joint properties in modelling jointed rock masses. Keynote lecture. In *Proceedings of the 8th ISRM Congress*, Tokyo, Japan, 25–29 September 1995; Volume 3, pp. 1023–1032.
35. Hoek, E.; Carter, T.G.; Diederichs, M.S. Quantification of the Geological Strength Index Chart. In *Proceedings of the 47th US Rock Mechanics/Geomechanics Symposium ARMA*, San Francisco, CA, USA, 23–26 June 2013; pp. 13–672.
36. Cai, M.; Kaiser, P.K. Visualization of rock mass classification systems. *Geotech. Geol. Eng.* **2006**, *24*, 1089–1102. [[CrossRef](#)]
37. Russo, G. A new rational method for calculating the GSI. *Tunn. Undergr. Space Technol.* **2009**, *24*, 103–111. [[CrossRef](#)]
38. Morelli, G.L. Variability of the GSI index estimated from different quantitative methods. *Geotech. Geol. Eng.* **2015**, *33*, 983–995. [[CrossRef](#)]

39. Sari, M. Incorporating variability and/or uncertainty of rock mass properties into GSI and RMi systems using Monte Carlo method. In *Engineering Geology for Society and Territory-Volume 6*; Lollino, G., Giordan, D., Thuro, K., Carranza-Torres, C., Wu, F., Marinos, P., Delgado, C., Eds.; Springer International Publishing: Berlin/Heidelberg, Germany, 2015; pp. 843–849.
40. Somodi, G.; Krupa, Á.; Kovács, L.; Vásárhelyi, B. Comparison of different calculation methods of Geological Strength Index (GSI) is a specific underground site. *Eng. Geol.* **2018**, *243*, 50–58. [[CrossRef](#)]
41. Coşar, S. Application of Rock Mass Classification Systems for Future Support Design of the Dim Tunnel Near Alanya. Ph.D. Thesis, Middle East Technical University, Ankara, Turkey, 2014.
42. Irvani, I.; Wilopo, W.; Karnawati, D. Determination of nuclear power plant site in west bangka based on rock mass rating and geological strength index. *J. Appl. Geol.* **2013**, *5*, 78–86.
43. Singh, J.L.; Tamrakar, N.K. Rock mass rating and geological strength index of rock masses of Thopal-Malekhu river areas, Central Nepal lesser Himalaya. *Bull. Dept. Geol.* **2013**, *16*, 29–42. [[CrossRef](#)]
44. Ali, W.; Mohammad, N.; Tahir, M. Rock mass characterization for diversion tunnels at Diamer Basha dam, Pakistan—A design perspective. *Int. J. Sci. Eng. Technol.* **2014**, *3*, 1292–1296.
45. Zhang, Q.; Huang, X.; Zhu, H.; Li, J. Quantitative assessments of the correlations between rock mass rating (RMR) and geological strength index (GSI). *Tunn. Undergr. Space Technol.* **2018**, *83*, 73–81. [[CrossRef](#)]
46. Siddique, T.; Khan, E.A. Stability appraisal of road cut slopes along a strategic transportation route in the Himalayas, Uttarakhand, India. *SN Appl. Sci.* **2019**, *1*, 409. [[CrossRef](#)]
47. Osgoui, R.; Ünal, E. Rock reinforcement design for unstable tunnels originally excavated in very poor rock mass. In Proceedings of the International World Tunnel Congress and the 31st ITA General Assembly, Istanbul, Turkey, 7–12 May 2005; pp. 291–296.
48. Deák, F.; Kovács, L.; Vásárhelyi, B. Geotechnical rock mass documentation in the Bábaapáti radioactive waste repository. *Centr. Eur. Geol.* **2014**, *57*, 197–211. [[CrossRef](#)]
49. Somodi, G.; Krupa, Á.; Kovács, L.; Szujó, G. Reviewing length, density, and orientation data of fractures in a granitic rock mass. In Proceedings of the 2018 ISRM European Rock Mechanics Symposium (EUROCK2018), St. Petersburg, Russia, 22–27 May 2018; Volume 2, pp. 439–445.
50. Kovács, L.; Kádár, B.; Krupa, Á.; Mészáros, E.; Pöszmet, T.; Rátkai, O.; Somodi, G.; Amigyáné Reisz, K.; Vásárhelyi, B. *The Revision and Upgrade of Geotechnical Interpretative Report*; Manuscript; RHKK-028/16; Puram (RHK Kft.): Budapest, Hungary, 2016. (In Hungarian)
51. Benedek, K.; Bóthi, Z.; Mező Gy Molnár, P. Compartmented flow at the Bábaapáti site in Hungary. *Hydrogeol. J.* **2009**, *17*, 1219–1232. [[CrossRef](#)]
52. Benedek, K.; Molnár, P. Combining hydrogeological and structural data: A conceptualization of a fracture system. *Eng. Geol.* **2013**, *163*, 1–10. [[CrossRef](#)]
53. Tóth, T.M. Determination of geometric parameters of fracture networks using 1D data. *J. Struct. Geol.* **2010**, *32*, 878–885. [[CrossRef](#)]
54. Bar, N.; Weekes, G. Directional Shear Strength Models in 2D and 3D Limit Equilibrium Analyses to Assess the Stability of Anisotropic Rock Slopes in the Pilbara Region of Western Australia. *Aust. Geomech.* **2017**, *52*, 91–104.
55. Bar, N.; Yacoub, T.E.; McQuillan, A. Analysis of a large open pit mine in Western Australia using finite element and limit equilibrium methods. In Proceedings of the 53rd US Rock Mechanics/Geomechanics Symposium ARMA, New York, NY, USA, 23–26 June 2019.